

# Lawrence Berkeley National Laboratory

## Recent Work

### Title

CALCULATED BAND STRUCTURES, OPTICAL CONSTANTS AND ELECTRONIC CHARGE DENSITIES FOR InAs AND InSb

### Permalink

<https://escholarship.org/uc/item/1qg842md>

### Author

Varea De Alvarez, Carmen.

### Publication Date

1972-01-01

Submitted to Physical  
Review

RECEIVED  
LIBRARY  
LAWRENCE BERKELEY

LBL-482 *e.2*  
Preprint

DOCUMENTS

CALCULATED BAND STRUCTURES, OPTICAL CONSTANTS AND  
ELECTRONIC CHARGE DENSITIES FOR InAs and InSb

Carmen Varea de Alvarez, John P. Walter,  
Robert W. Boyd and Marvin L. Cohen

January 1972

AEC Contract No. W-7405-eng-48

**TWO-WEEK LOAN COPY**

**This is a Library Circulating Copy  
which may be borrowed for two weeks.  
For a personal retention copy, call  
Tech. Info. Division, Ext. 5545**



LBL-482

*e.2*

## **DISCLAIMER**

This document was prepared as an account of work sponsored by the United States Government. While this document is believed to contain correct information, neither the United States Government nor any agency thereof, nor the Regents of the University of California, nor any of their employees, makes any warranty, express or implied, or assumes any legal responsibility for the accuracy, completeness, or usefulness of any information, apparatus, product, or process disclosed, or represents that its use would not infringe privately owned rights. Reference herein to any specific commercial product, process, or service by its trade name, trademark, manufacturer, or otherwise, does not necessarily constitute or imply its endorsement, recommendation, or favoring by the United States Government or any agency thereof, or the Regents of the University of California. The views and opinions of authors expressed herein do not necessarily state or reflect those of the United States Government or any agency thereof or the Regents of the University of California.

Calculated Band Structures, Optical Constants and  
Electronic Charge Densities for InAs and InSb.\*

Carmen Varea de Alvarez,<sup>†</sup> John P. Walter,<sup>\*\*</sup> Robert W. Boyd  
and Marvin L. Cohen

Department of Physics, University of California

and

Inorganic Materials Research Division, Lawrence Berkeley Laboratory

Berkeley, California 94720

Abstract

The energy band structure, reflectivity, modulated reflectivity and imaginary part of the frequency dependent dielectric function are calculated for InAs and InSb using the empirical pseudopotential method. Comparison is made with the measured reflectivity and modulated reflectivity and prominent features in the experimental spectra are identified and associated with interband transitions in specific regions of the Brillouin zone. The wavefunctions

---

\* Supported in part by the National Science Foundation Grant GP 13632

<sup>†</sup> Consejo Nacional de Ciencia y Tecnologia, Mexico

<sup>\*\*</sup> Present address: Department of Physics, Brandeis University, Waltham, Massachusetts 02154.

obtained from our calculated band structures are used to calculate the electronic charge density as a function of position in the unit cell.

### Introduction

The empirical pseudopotential method<sup>1,2</sup> (EPM) employs the use of optical data to obtain one-electron potentials which can then be used to calculate energy bands and optical constants. In this paper we have applied this method to analyze the electronic structure of InAs and InSb. The availability of new optical data, particularly modulated reflectivity data<sup>3</sup> (and the inclusion of spin-orbit interactions) allow a more accurate determination of the band structure than in earlier work.<sup>2</sup>

Since we are only concerned with direct transitions in interpreting the reflectivity and in fitting the band structure, we expect that the direct energy gaps at the points of interest in the Brillouin zone will be accurate, whereas the indirect gaps may not. Comparisons of the calculated and measured spectra show that our model gives the correct energies for the prominent optical structure to the order of 1/4 eV. These comparisons also allow us to identify the interband transitions responsible for the prominent structure in the reflectivity.

After a brief discussion of the calculation we present the results for the band structure; reflectivity,  $R(\omega)$ ; modulated reflectivity,  $\frac{1}{R} \frac{dR(\omega)}{d\omega}$ ; and the imaginary part of the frequency dependent dielectric function,  $\epsilon_2(\omega)$ , for both InAs and InSb. In the calculations we implicitly assume a temperature

of 5K which is the temperature at which the modulated reflectivity spectra was measured.

### Calculation

The calculation is based on the EPM. If the crystal potential is expanded in the reciprocal lattice, it can be expressed in terms of a structure factor,  $S(\vec{G})$ , and form factors  $V_a(G)$  of the atomic potential

$$V(\vec{r}) = \sum_G V(G) e^{i\vec{G} \cdot \vec{r}} \quad (1)$$

$$V(G) = \sum_a S(\vec{G}) V_a(G) \quad (2)$$

$$S(\vec{G}) = e^{i\vec{G} \cdot \vec{\tau}_a} \quad (3)$$

where  $\vec{\tau}_a$  is the vector which locates each atom in a cell.

This potential can then be used to calculate the energy levels.<sup>1,2</sup> The input is the structure factor which can be obtained from x-ray analysis and the  $V_a(G)$ 's. The EPM involves the use of optical data to obtain the  $V_a(G)$ 's. Usually three form factors are all that is required for each atom. Calculated values for these form factors can be used, then the optical spectrum can be calculated. In general the peaks calculated this way will be shifted from those in the experimental curves. Adjustment of the form factors can move the peaks until a good fit is obtained. This is the basis of the EPM and accurate spectra can be calculated.<sup>4</sup> For the optical spectra analysis the dielectric function  $\epsilon(q=0, \omega)$  is calculated. It is also possible to calculate  $\epsilon(q, \omega=0)$ <sup>5</sup>. If the calculated  $\epsilon(q)$  is used to screen

a bare atomic potential, the resulting potential<sup>5</sup> is close to that obtained using the EPM. This self-consistency is reassuring.

Both InAs and InSb crystallize in the zincblende structure. Application of the EPM to this structure is well-documented<sup>1,2,4</sup> so we will not repeat the details here. The form factors were obtained by first starting with the form factors of reference 2 and then varying them to obtain a modulated reflectivity spectrum in agreement with experiment. The variation of the form factors was at most 0.055 Ry.

The spin-orbit interaction is included using the method of Weisz<sup>6</sup> as modified by Bloom and Bergstresser.<sup>7</sup> Two spin-orbit parameters are used to characterize the spin-orbit interaction.<sup>8</sup> The metallic form factor is allowed to vary from its free atomic value, while the non-metallic parameter is constrained so as to maintain a constant ratio between the two parameters. This constant ratio is set equal to the ratio of the spin-orbit interactions for the two atoms as determined by Herman and Skillman.<sup>9</sup> Using this one arbitrary parameter, we are able to obtain the experimentally known splittings at  $\Gamma$  and L to within 0.05 eV.

Table I compares the Cohen and Bergstresser (CB) form factors<sup>2</sup> with those used in the present calculation. The pseudopotential form factors are changed by less than 0.05 Ry for InAs and 0.055 Ry for InSb. In the CB calculations, the symmetric form factors of InSb were constrained to be the same as the form factors for Sn, and the symmetric form factors for InAs were constrained to be the average of the form factors for Ge and Sn. We did not impose this constraint in the present calculation.

## Results

The calculated energy bands for InAs and InSb are given in Figs. 1 and 5. These are similar to other energy band calculations<sup>7,10</sup> for these materials. Using the calculated energy bands throughout the Brillouin zone, the imaginary part of the frequency-dependent dielectric function,  $\epsilon_2(\omega)$ , can be computed.<sup>1</sup> This function can then be used to compute the reflectivity,  $R(\omega)$ , and the modulated reflectivity,  $R'(\omega)/R(\omega)$  as shown in reference 1. The sharp structure in  $\epsilon_2(\omega)$ ,  $R(\omega)$  and  $R'/R$  arises from Van Hove<sup>11,1</sup> singularities in the joint density of states between the valence and conduction bands. These singularities arise when the gradient with respect to  $\vec{k}$  of the energy bands  $E(k)$  are equal for the conduction and valence bands of interests. There are four types of singularities in three dimensions<sup>1,11</sup> a minimum  $M_0$ , a maximum  $M_3$  and two saddle points  $M_1$  and  $M_2$ .

Figs. 2 and 6 contain the theoretical imaginary part of the frequency dependent dielectric function for InAs and InSb. The calculated and measured<sup>12,13</sup> reflectivities appear in Figs. 3 and 7 for these crystals. The calculated and measured<sup>3</sup> modulated spectra for InAs and InSb appear in Figs. 4 and 8. Tables II and III compare the energies of the prominent structure in the calculated and measured curves for InAs and InSb. These tables also give the origin in the Brillouin zone for the interband transitions which give rise to the optical structure, the critical point (cp) energy, i. e. the interband energy at which a Van Hove singularity is found, and the symmetry of the associated Van Hove singularity. In some cases a cp is not discernible, and the structure arises from transitions in a volume of the zone; these are labelled in the table.

The two crystals will be discussed separately.

### InAs

The first direct gap (Fig. 1) is  $\Gamma_8 - \Gamma_6$ .<sup>14</sup> The measured gap is 0.42 eV;<sup>15</sup> the  $\Gamma$  spin orbit splitting ( $\Gamma_7 - \Gamma_8$ ) is also 0.42 eV.<sup>16,3</sup> The spin-orbit splitting near  $L(L_6 - L_4L_5)$  is 0.27 eV.<sup>3</sup> In the calculated curves the spin-orbit parameter for In was adjusted to give a L splitting of 0.27 eV. The calculated splitting at  $\Gamma$  is 0.40 eV.

The calculated  $\Gamma_8 - \Gamma_6$  transitions give rise to the  $M_0$  threshold in  $\epsilon_2(\omega)$ , (Fig. 2), at 0.46 eV. The  $\Gamma_7 - \Gamma_6$  threshold at 0.86 eV is hidden in the background. These transitions give rise to a slight bump in  $R(\omega)$ , (Fig. 3); however, both transitions show up in the calculated  $R'(\omega)/R(\omega)$  spectrum (Fig. 4).

The first peak in  $\epsilon_2(\omega)$  occurs at 2.60 eV and is caused by L(4-5) and  $\Lambda$ (4-5) transitions.<sup>14</sup> The spin-orbit split peak at 2.90 eV is caused by L(3-5) and  $\Lambda$ (3-5) transitions. This structure gives rise to peaks in the reflectivity spectrum at 2.58 eV and 2.85 eV which agree favorably with the experimental values of 2.61 and 2.88 eV.

The small shoulder at 4.45 eV on the lower side of the main peak in  $\epsilon_2(\omega)$  is caused by (4-5) transitions at X and along  $\Delta$ (3-5). The corresponding structure in the calculated reflectivity is at 4.47 eV, whereas the measured value is 4.58 eV.  $\Delta$ (4-5) and  $\Gamma$ (4-6) transitions just below this energy show up in the experimental  $R'/R$  spectra at 4.39 eV and correspond to the small structure at 4.37 eV of the theoretical  $R'/R$  curve at 4.63 eV. Excitonic effects at  $\Gamma$  may enhance the experimental spectrum.

The main peak in  $\epsilon_2(\omega)$  occurs at 4.63 eV and this peak comes from  $\Sigma(4-5)$  transitions at 4.65 eV. Transitions near X(4-5) also add to the height of the main peak. The main peak in the calculated reflectivity occurs at 4.7 eV; the experimental value is 4.74 eV. On the high energy side of the main peak in  $\epsilon_2(\omega)$ , there are two changes in slope at about 5.32 eV, and at 5.35 eV. The first structure comes from  $\Delta(4-6)$  transitions at 5.25 eV; this structure is found in the calculated reflectivity at 5.3 eV, close to the experimental value of 5.31 eV. The second structure arises mainly from  $\Delta(3-6)$  transitions at 5.39 eV. The peak in the calculated reflectivity occurs at 5.57 eV, while the measured value is 5.5 eV.

Critical points at  $\Lambda(4-7)$  and  $L(4-7)$  with energies of 5.91 eV and 5.96 eV cause the next peak in  $\epsilon_2(\omega)$ . The peak in the calculated reflectivity occurs at 6.05 eV. The experimental value for this peak is 6.5 eV, and is obtained by correcting the original value of 6.4 eV at 300<sup>o</sup>K to the low temperature limit, the agreement here is only fair.

The next small peak in  $\epsilon_2(\omega)$  at 6.4 eV is caused by  $\Lambda(3-7)$  transitions of 6.23 eV. It's counterpart in the measured reflectivity is a broad peak at 6.44 eV, the experimental value for this peak is 6.8 eV. The last structure which can be accurately identified is the shoulder at 7.1 eV, coming from (4-7) transitions in the energy range near 7.1 eV. The peak in the calculated reflectivity occurs at 7.3 eV, the corresponding temperature adjusted experimental value is 7.1 eV.

### InSb

The measured splitting of the first direct gap for InSb,  $\Gamma_8 - \Gamma_6$  is 0.24 eV;<sup>17</sup> the spin orbit splitting at the top of the valence band at  $\Gamma$  is 0.82 eV<sup>18,3</sup> and 0.50 eV<sup>18,3</sup> at L. The calculated band structure is plotted in

Fig. 5; the  $\Gamma_8 - \Gamma_6$  splitting is 0.23 eV. The spin-orbit parameter for In is adjusted to give a splitting of 0.82 eV at  $\Gamma$  and the calculated value at L is 0.55 eV.

The imaginary part of the dielectric function, the calculated reflectivity and the calculated modulated reflectivity are given in Figs. 6, 7, and 8 respectively. The  $\Gamma_8 - \Gamma_6$  transitions give rise to the threshold in  $\epsilon_2(\omega)$  at 0.26 eV. The spin-orbit split transition  $\Gamma_7 - \Gamma_6$  gives a small peak in  $\epsilon_2(\omega)$ , but this is largely masked by fluctuations inherent in the calculation. Both contributions appear clearly in the calculated  $R'/R$  curve at 0.26 eV and 0.66 eV respectively.

The first peak in  $\epsilon_2(\omega)$  at 1.98 eV is caused by  $\Lambda(4-5)$  transitions at 1.94 eV. The next peak at 2.6 eV is caused by  $\Lambda(3-5)$  transitions at 2.5 eV. Associated with these structures are the spin-orbit split  $\Lambda$  peaks in the reflectivity at 2.03 eV and 2.6 eV. The positions of these peaks agree well with the experimental values of 1.98 eV and 2.48 eV.

The rise at 3.55 eV on the low side of the main peak in  $\epsilon_2(\omega)$  arises from (4-5) transitions in a volume located near  $\Delta$ . At slightly higher energies near the main peak, there is a shoulder at 3.8 eV. This shoulder is caused by  $\Delta(3-5)$  transitions at 3.83 eV. In the reflectivity spectrum, these features give rise to a shoulder at 3.65 eV and a shoulder at 3.83 eV. The experimental values are 3.39 eV and 3.78 eV.

The main peak in  $\epsilon_2(\omega)$  is caused primarily by  $\Sigma(4-5)$  transitions at 4.1 eV. This structure gives rise to the peak at 4.01 eV in the reflectivity. This peak occurs lower in energy than at the experimental value of 4.23 eV.

The small structure and peak on the high side of the main peak in  $\epsilon_2(\omega)$  at 4.4 and 4.75 eV are caused by (4-6) transitions in a volume of k-space at about 4.4 eV and by  $\Delta(4-6)$  transitions at 4.75 eV. These are related to the two bumps in the reflectivity at 4.48 and 4.73 eV. These energies are in good agreement with the experiment.

The peak at 4.8 eV and the small shoulder at 5.09 eV in the  $\epsilon_2(\omega)$  curve are caused by  $\Lambda(4-6)$ ,  $\Delta(3-6)$  and  $\Lambda(3-6)$  transitions at 4.87 eV, 4.94 eV and 5.43 eV. The related reflectivity structures are the broad peak at 5.3 eV with a highly blurred shoulder at 4.73 eV; the corresponding experimental values are at 5.33 and 4.92 eV.

The peak in  $\epsilon_2(\omega)$  at 5.73 eV arises mainly from  $\Lambda(3-7)$  transitions at 5.69 eV. The peak in  $R(\omega)$  is at 6.01 eV, in good agreement with the experimental value of 5.96 eV.

As for the  $\Gamma_6^c - \Gamma_7^c$ ,  $\Gamma_6^c - \Gamma_8^c$  doublet, electroreflectance measurements in n-type InSb<sup>19</sup> show two peaks at 3.16 and 3.54 eV with a red shift response to an increase of the surface potential; this structure disappears as the conduction band is depopulated. These two facts indicate that these two peaks come from transitions from the top of the conduction band ( $\Gamma_6^c$ ) to higher conduction bands ( $\Gamma_7^c$  and  $\Gamma_8^c$ ). Since these are s-like to p-like transitions, we expect that the oscillator strengths for these transitions are strong enough to be observable. Our calculated energy differences are

$$\Gamma_6^c - \Gamma_7^c = 2.43 \text{ eV} ; \quad \Gamma_6^c - \Gamma_8^c = 3.41 \text{ eV}$$

in fair agreement with the experimental values.

Most of the above assignments for both InAs and InSb are consistent with those of references 1, 3 and 20.

### Electronic Charge Densities

We have solved the secular equation for the pseudopotential Hamiltonian for the wavefunctions  $\psi_{n,\mathbf{k}}(\mathbf{r})$  on a grid of 3360 points in the Brillouin zone ( $n$  is the band index)<sup>21</sup> for InAs and InSb. From these wavefunctions we obtain the charge density in each valence band as

$$\rho_n(\vec{r}) = \sum_{\vec{k}} e |\psi_{n,\vec{k}}(\vec{r})|^2 .$$

Figs. 10 and 11 show the contour maps of the sum over the first four valence bands for InAs and InSb respectively, for the plane (1, -1, 0) as shown in Fig. 9. The density is plotted in units of  $(e/\Omega)$  where  $\Omega$  is the volume of the primitive cell,  $\Omega = a^3/4$ .

Our results are consistent with the fact that InAs is a more ionic crystal than InSb,<sup>22</sup> the charge being more piled up towards the As atom in InAs than towards the Sb atom in InSb.

The form factors used here for InSb are different from those used in reference 21 and give a much better agreement with the optical data. We have calculated the covalent bonding charge  $Z_b$  as described. Our result is  $Z_b = 0.083 e$ . When this result is plotted using Phillips and Van Vechten<sup>22</sup> ionicity scale with earlier results for Sn and CdTe, the curve of bonding charge versus ionicity is more linear, but the extrapolated value of the critical ionicity  $f_c$  does not change when compared with the results of Walter and Cohen.<sup>21</sup>

The value for  $Z_b$  we obtain for InAs is 0.069e. When this is plotted vs. the ionicity scale of Phillips and Van Vechten, this point lies very near the curve of the Ge family of Walter and Cohen.

#### References

1. M. L. Cohen and V. Heine, Solid State Physics 24, ed. H. Ehrenreich, F. Seitz and D. Turnbull (Academic Press, Inc., New York, N. Y., 1970), p. 37.
2. M. L. Cohen and T. K. Bergstresser, Phys. Rev. 141, 789 (1966).
3. R. R. L. Zucca and Y. R. Shen, Phys. Rev. B1, 2668 (1970).
4. J. P. Walter and M. L. Cohen, Phys. Rev. 183, 763 (1969).
5. J. P. Walter and M. L. Cohen, Phys. Rev. B2, 1821 (1970).
6. G. Weisz, Phys. Rev. 149, 504 (1966).
7. S. Bloom and T. K. Bergstresser, Solid State Comm. 6, 465 (1968).
8. J. P. Walter, M. L. Cohen, Y. Petroff, and M. Balkanski, Phys. Rev. E1, 2661 (1970).
9. F. Herman and Skillman, "Atomic Structure Calculations", (Prentice-Hall, Inc., Englewood Cliffs, N. J., 1963).
10. C. W. Higginbotham, F. H. Pollak, and M. Cardona, in "Proceedings of the Ninth International Conference on the Physics of Semiconductors, Moscow" (Nauka, Leningrad, 1968), p. 57. F. Herman, R. L. Kortum, C. D. Kuglin, and J. P. Van Dyke, "Methods in Computational Physics", eds. R. Adler, S. Fernbach, and M. Rotenberg, (Academic Press, Inc., N. Y., 1968).
11. L. Van Hove, Phys. Rev. 89, 1189 (1953).

12. H. Ehrenreich, H. R. Philipp and J. C. Phillips, Phys. Rev. Letters 8, 59 (1962). The values have been adjusted to a temperature of 5K.
13. S. S. Vishnubhatla and J. C. Woolley, Canad. J. Phys. 46, 1769 (1968).
14. In discussing gaps or transitions the valence band is listed first, then the conduction band, e.g.  $\Gamma_8 - \Gamma_6$  means  $\Gamma_8$ (valence) and  $\Gamma_6$ (conduction). Another notation will also be used, e.g.  $\Lambda(4-5)$  means a transition occurring between bands 4 and 5 (small splittings like those found along  $\Gamma - K$  not included) at the  $\Lambda$  point in the Brillouin zone. The first valence band is labelled 1; the first conduction band is 5.
15. J. R. Dixon and J. M. Ellis, Phys. Rev. 123, 1560 (1961).
16. F. Matossi and F. Stern, Phys. Rev. 111, 472 (1958).
17. H. Ehrenreich, J. Appl. Phys. Suppl. 32, 2155 (1961).
18. M. Cardona, K. L. Shalkee and F. H. Pollak, Phys. Rev. 154, 696 (1967).
19. R. Glosser, J. E. Fischer, and B. O. Seraphin, Phys. Rev. B1, 1607 (1970).
20. R. N. Cahn and M. L. Cohen, Phys. Rev. B1, 2569 (1970).
21. J. P. Walter and M. L. Cohen, Phys. Rev. B4, 1877 (1971).
22. J. C. Phillips, Rev. Mod. Phys. 42, 317 (1970).

Table Captions

- Table 1 A comparison of the form factor ( $R_y$ ) of Cohen and Bergstresser (Ref. 2) with the form factors used in the present calculation. The lattice constants are also given.
- Table 2 Identification of transitions responsible for the prominent theoretical and experimental reflectivity structure in InAs, including location in the Brillouin zone, energy, and symmetry of the calculated critical points.
- Table 3 Identification of transitions responsible for the prominent theoretical and experimental reflectivity structure in InSb including location in the Brillouin zone, energy, and symmetry of the calculated critical points.

Table I

	InAs		InSb	
	Cohen and Bergstresser <sup>a</sup>	Present Work	Cohen and Bergstresser <sup>a</sup>	Present Work
lattice constant	6.04A	6.053 <sup>b</sup>	6.48	6.473 <sup>b</sup>
V(3)	-0.22Ry	-0.2699	-0.20	-0.2547
V(8)	0.0	.0196	0.0	.0188
V(11)	0.05	.0411	0.04	.0452
V(3)	0.08	.0775	0.06	.0302
V(4)	0.05	.0384	0.05	.0012
V(11)	0.03	.0364	0.01	.0329
metallic spin-orbit parameter	-	0.00137	-	0.00203
non-metallic spin-orbit parameter	-	0.00109	-	0.00260

a) M. L. Cohen and T. K. Bergstresser, Phys. Rev. 141, 789 (1966).

b) Y. G. Giesecke and H. Pfister, Acta. Cryst. 11, 369 (1958). S. I. Novikova, Soviet Physics Solid State 2, 2087 (1961). Lattice constants were scaled to a temperature of 5K.

Table II

Reflectivity Structure		Associated Critical Points (InAs)		
Theory	Exper. (a)	Location in zone	Symmetry	$c_p$ energy
0.46 eV	0.42 eV	$\Gamma(4-5)(0,0,0)$	$M_0$	0.46 eV
2.58	2.61	$\Lambda(4-5)(0.3,0.3,0.3)$	$M_1$	2.47
		$L(4-5)(0.5,0.5,0.5)$	$M_1$	2.48
2.85	2.88	$\Lambda(3-5)(0.3,0.3,0.3)$	$M_1$	2.74
		$L(3-5)(0.5,0.5,0.5)$	$M_1$	2.75
4.37	4.39	$\Delta(4-5)(0.7,0,0)$	$M_1$	4.3
		$\Gamma(4-6)(0,0,0)$	-	4.37
4.47	4.58	$X(4-5)(1.0,0,0)$	$M_1$	4.43
		vol. near $(3-5)(0.7,0,0)$	-	4.43
4.7	4.74	$\Sigma(4-5)(0.7,0.7,0)$	$M_2$	4.65
		$\Delta(3-6)(0.3,0,0)$	$M_1$	4.69
5.3	5.31	vol. near $\Delta(4-6)(0.7,0,0)$	-	5.25
5.57	5.5	vol. near $\Delta(3-6)(0.7,0,0)$	-	5.39
6.05	6.5	$L(4-7)(0.5,0.5,0.5)$	$M_0$	5.91
		$\Lambda(4-7)(0.4,0.4,0.4)$	$M_1$	5.96
6.44	6.8 <sup>(c)</sup>	$L(3-7)(0.5,0.5,0.5)$	$M_0$	6.18
		$\Lambda(3-7)(0.4,0.4,0.4)$	$M_1$	6.23
7.37	7.1 <sup>(c)</sup>	vol. near $(4-7)(0.4,0.3,0.1)$	-	7.05

(a) R. R. L. Zucca and Y. R. Shen, Phys. Rev. B1, 2668 (1970), except as listed below.

(b) I. R. Dixon and J. M. Ellis, Phys. Rev. 123, 1560 (1961).

(c) H. Ehrenreich, H. R. Phillip, and J. C. Phillips, Phys. Rev. Letters 8, 59 (1962). These values have been adjusted to a temperature of 5K.

Table III

Reflectivity Structure		Associated Critical Points (InSb)		
Theory	Exper. <sup>(a)</sup>	Location in zone	Symmetry	$c_p$ energy
0.26 eV	0.24 eV <sup>(b)</sup>	$\Gamma(4-5)(0, 0, 0)$	$M_0$	0.26 eV
2.03	1.98	$\Lambda(4-5)(0.3, 0.3, 0.3)$	$M_1$	1.94
		$L(4-5)(0.5, 0.5, 0.5)$	$M_1$	2.0
2.60	2.48	$\Lambda(3-5)(0.3, 0.3, 0.3)$	$M_1$	2.5
		$L(3-5)(0.5, 0.5, 0.5)$	$M_1$	2.55
3.65	3.39	$\Delta(4-5)(0.7, 0, 0)$	$M_1$	3.65
3.83	3.78	$\Delta(3-5)(0.7, 0, 0)$	$M_1$	3.83
4.15	4.23	$\Delta(3-6)(0.2, 0, 0)$	$M_1$	3.95
		$\Sigma(4-5)(0.7, 0.7, 0)$	$M_2$	4.1
4.48	4.56	vol. near $\Delta(4-6)(0.5, 0, 0)$	-	4.4
4.73	4.75	$\Delta(4-6)(0.7, 0, 0)$	$M_3$	4.75
4.95	4.92	$L(4-6)(0.5, 0.5, 0.5)$	$M_0$	4.86
		$\Lambda(4-6)(0.4, 0.4, 0.4)$	$M_1$	4.87
		$\Delta(3-6)(0.7, 0, 0)$	$M_3$	4.94
5.3	5.33	$L(3-6)(0.5, 0.5, 0.5)$	$M_0$	5.41
		$\Lambda(3-6)(0.4, 0.4, 0.4)$	$M_1$	5.43
6.01	5.96	$L(3-7)(0.5, 0.5, 0.5)$	$M_0$	5.64
		$\Lambda(3-7)(0.4, 0.4, 0.4)$	$M_1$	5.69

(a) R. R. L. Zucca and Y. R. Shen, Phys. Rev. B1, 2668 (1970), except for b.

(b) H. Ehrenreich, J. Appl. Phys. Suppl. 32, 2155 (1961).

Figure Captions

- Fig. 1 Electronic band structure of InAs along the principal symmetry directions in the Brillouin zone. Some bands slightly split by spin-orbit interaction are drawn as degenerate because of the smallness of the splitting.
- Fig. 2 Calculation of the imaginary part of the frequency dependent dielectric function for InAs.
- Fig. 3 Calculated and measured reflectivity for InAs. Experiment 1 is H. Ehrenreich, H. R. Philipp, and J. C. Phillips, Phys. Rev. Letters 8, 59 (1962). Experiment 2 is S. S. Vishnubhatla and J. C. Woolley, Canad. J. Phys. 46, 1769 (1968).
- Fig. 4 Comparison of the theoretical and experimental modulated reflectivity spectrum for InAs. The experimental spectrum is from R. R. L. Zucca and Y. R. Shen, Phys. Rev. B1, 2668 (1970). Prominent structure is identified.
- Fig. 5 Electronic band structure of InSb along the principal symmetry directions in the Brillouin zone. Some bands slightly split by spin-orbit interaction are drawn as degenerate because of the smallness of the splitting.
- Fig. 6 Calculation of the imaginary part of the frequency dependent dielectric function for InSb.
- Fig. 7 Calculated and measured reflectivity for InSb. Experiment 1 is H. Ehrenreich, H. R. Philipp, J. C. Phillips, Phys. Rev. Letters 8, 59 (1962). Experiment 2 is S. S. Vishnubhatla and J. C. Woolley, Canad. J. Phys. 46, 1769 (1968).

- Fig. 8 Comparison of the theoretical and experimental reflectivity spectrum for InSb. The experimental spectrum is from R. R. L. Zucca and Y. R. Shen, Phys. Rev. B1, 2668 (1970). Prominent structure is identified.
- Fig. 9 Location of atoms in the primitive cells. A section of the (1, -1, 0) plane is shown bounded by dashed lines.
- Fig. 10 InAs charge density--sum of valence bands 1-4.
- Fig. 11 InSb charge density--sum of valence bands 1-4.

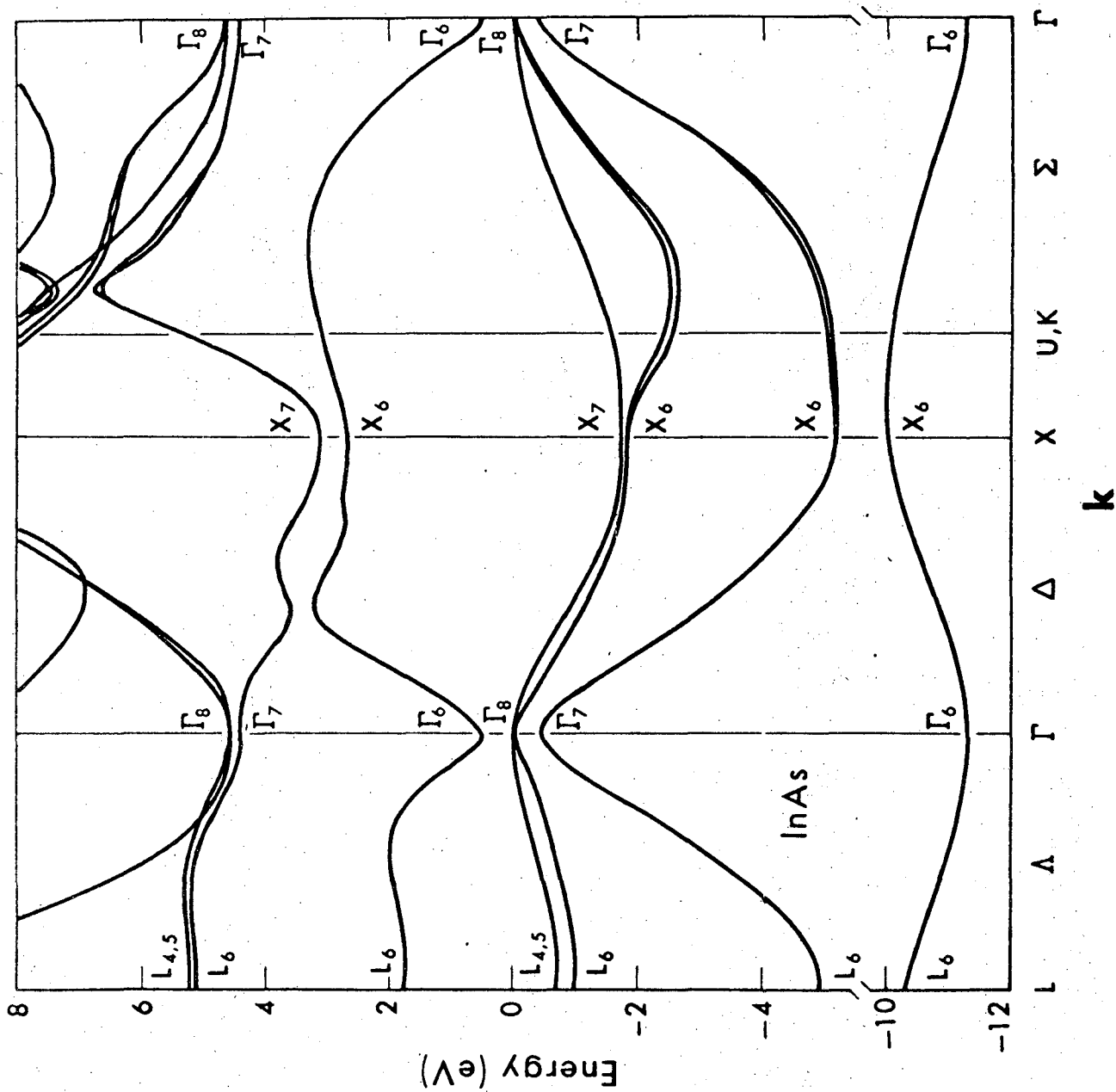


FIG. 1

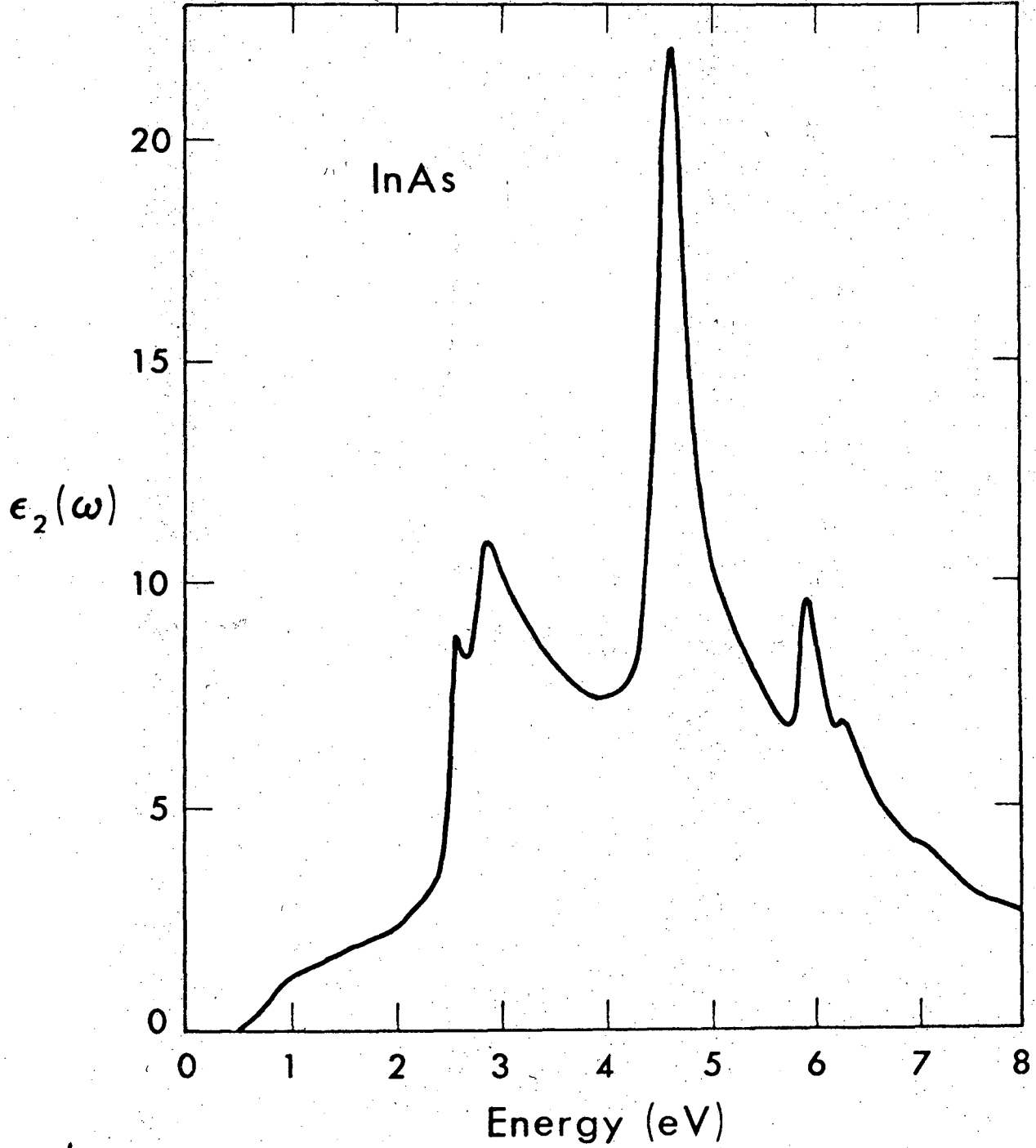


Fig. 2

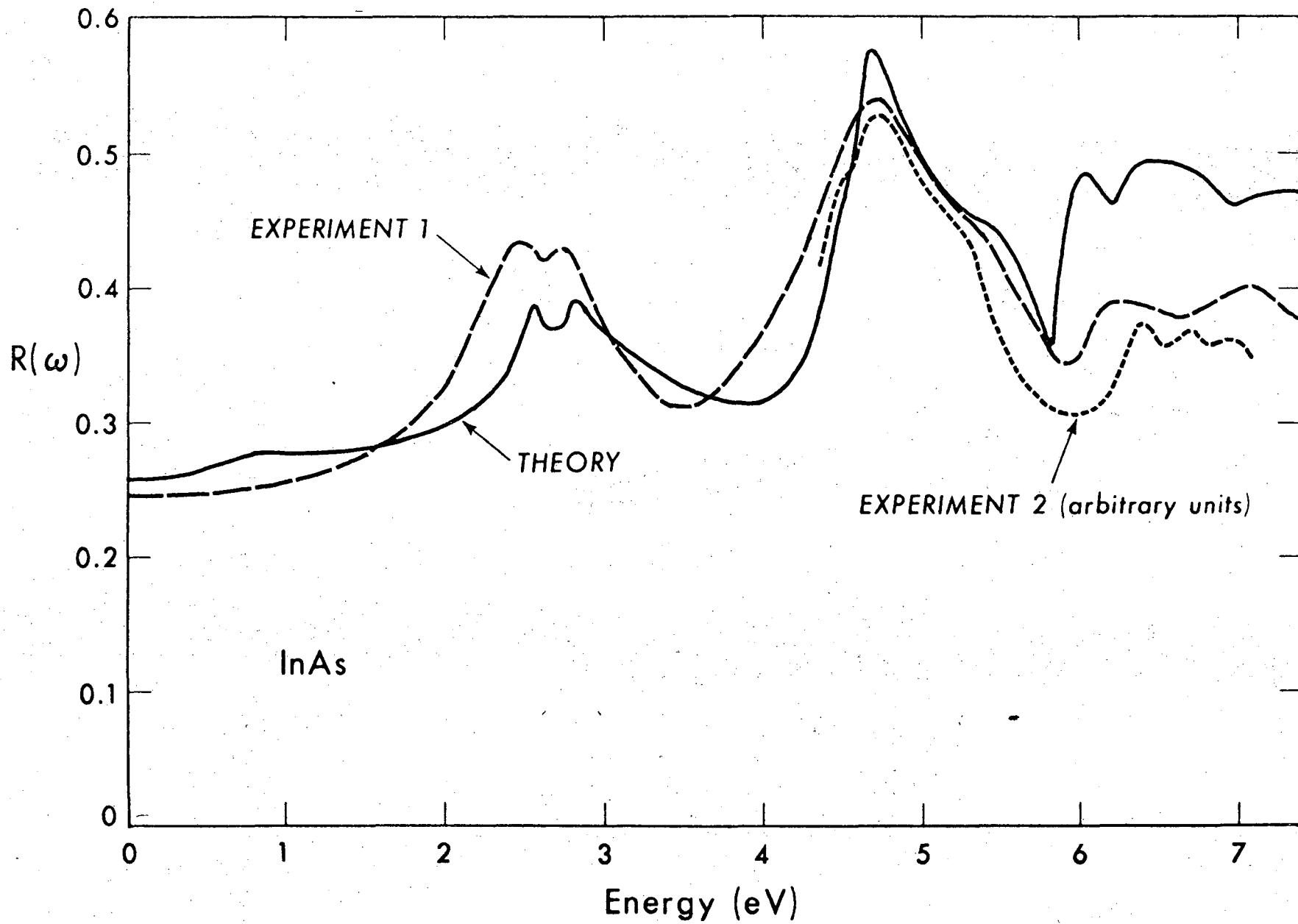
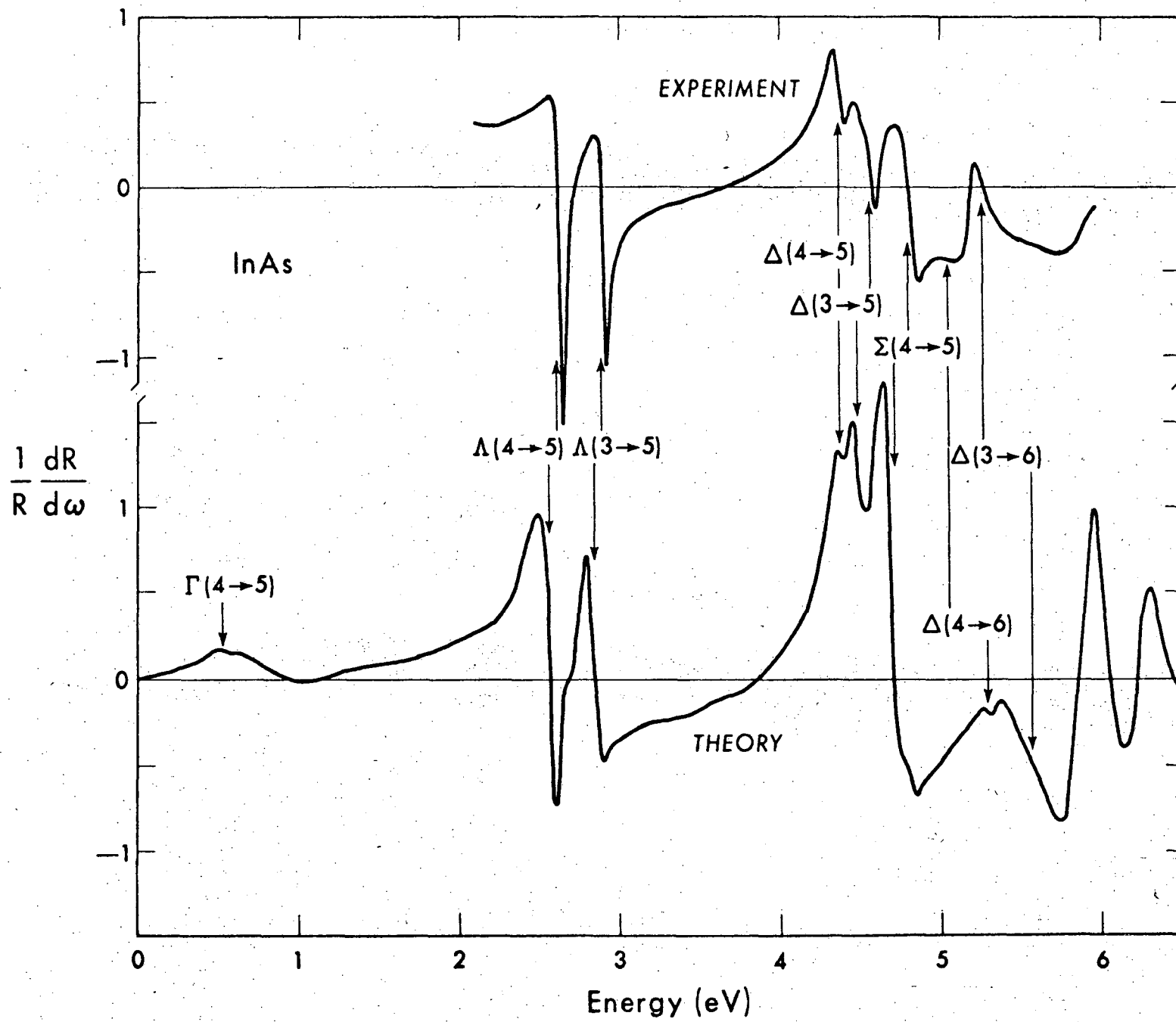


Fig. 3



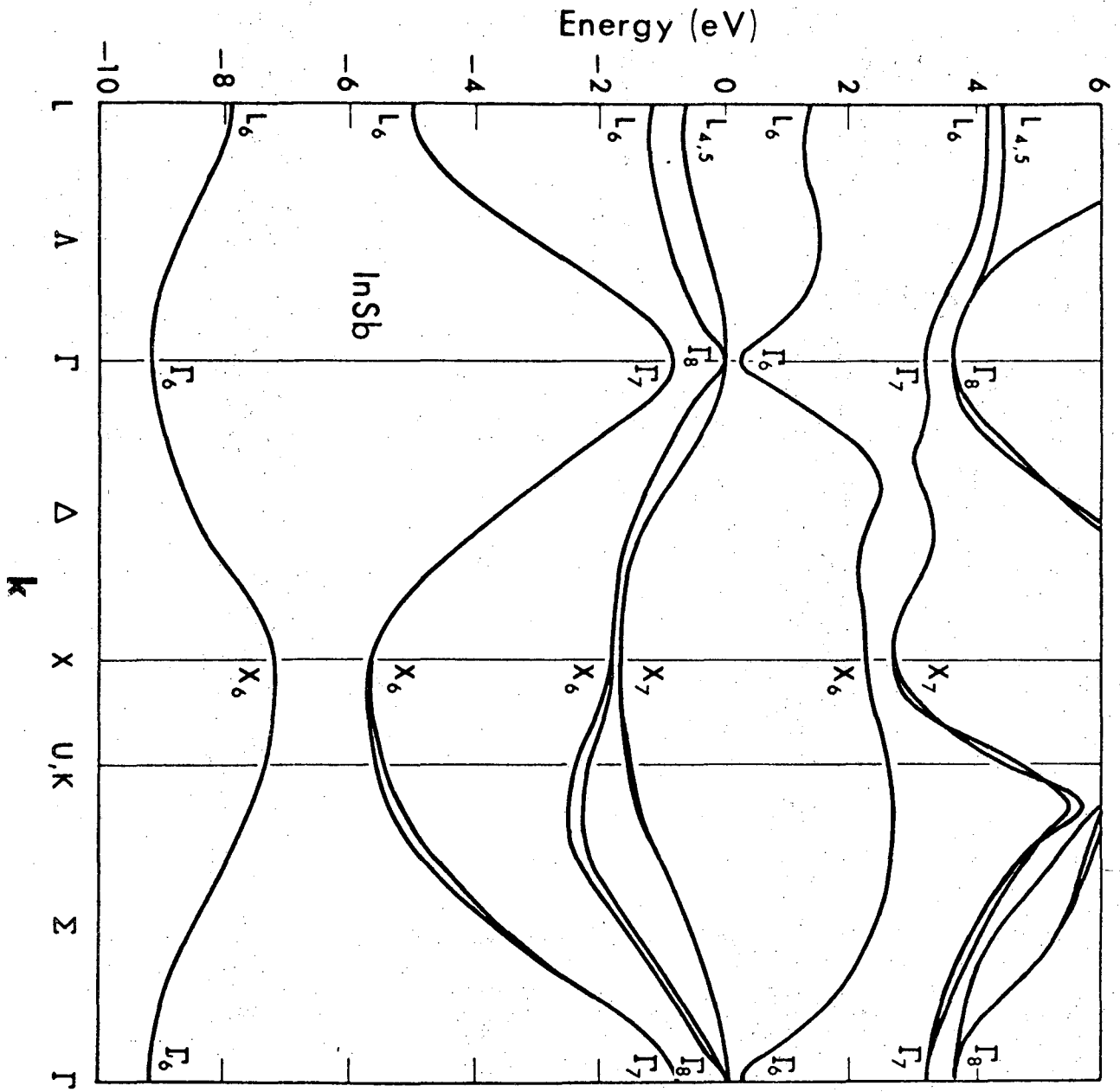


Fig. 5

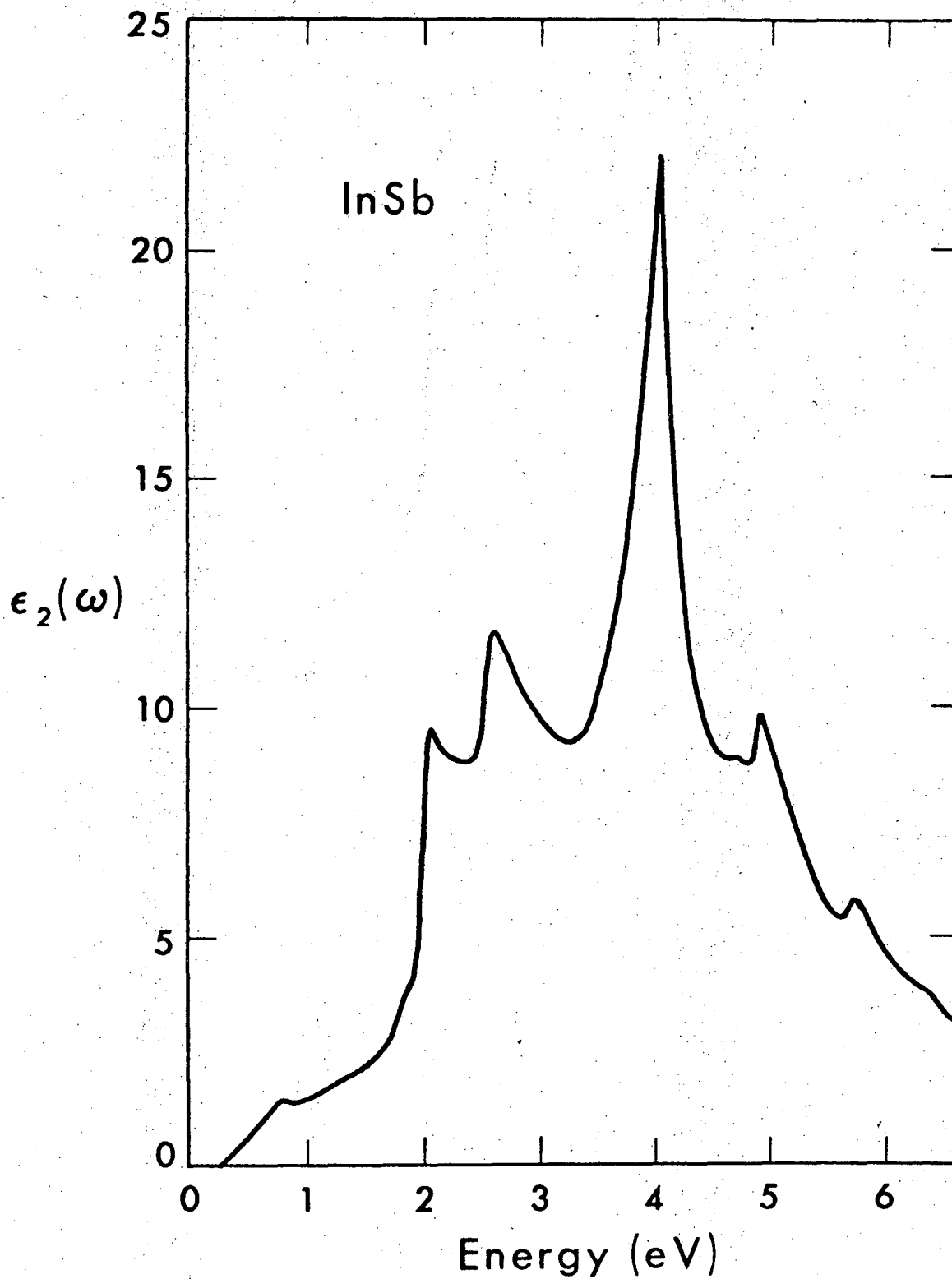


Fig. 6

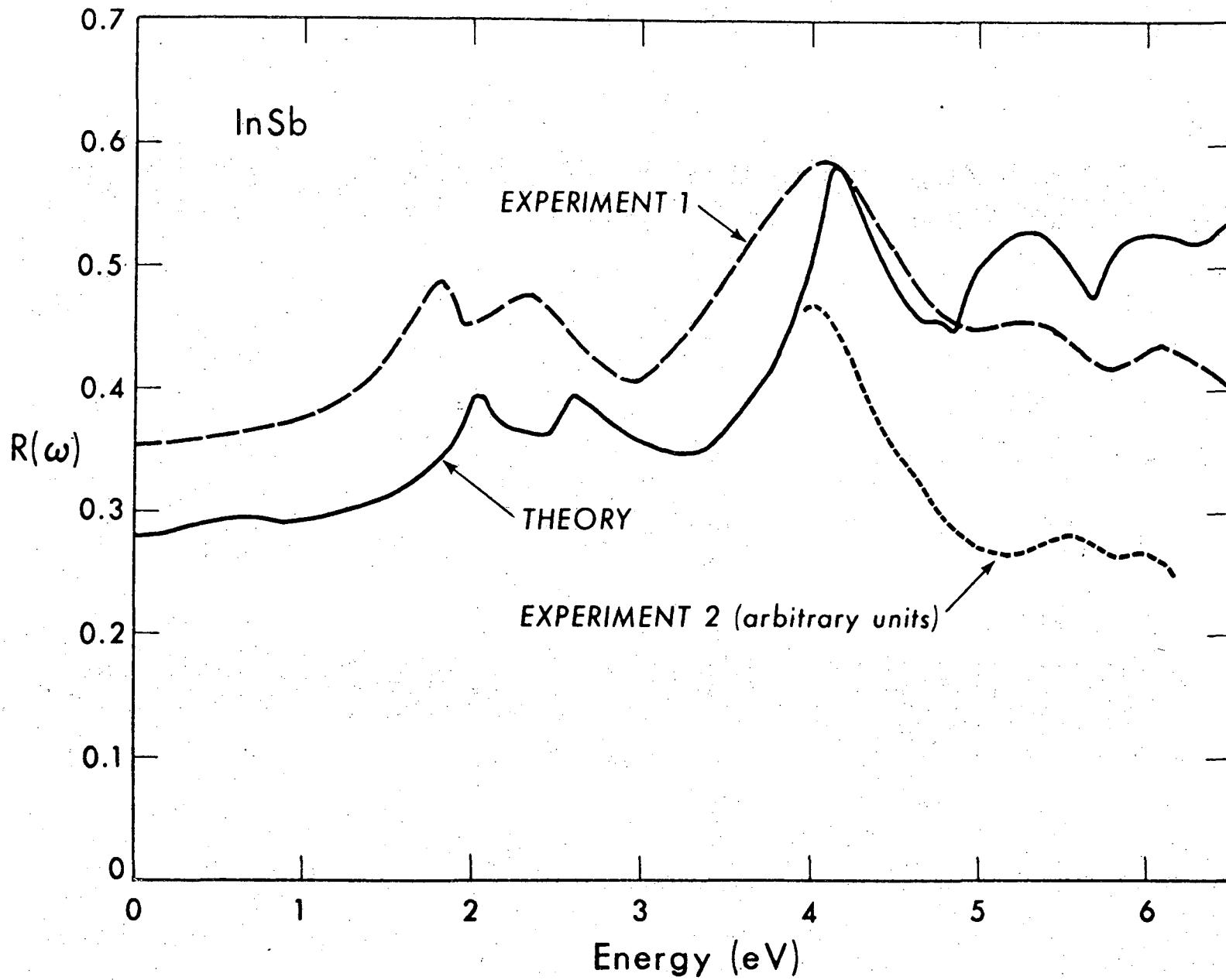


Fig. 7

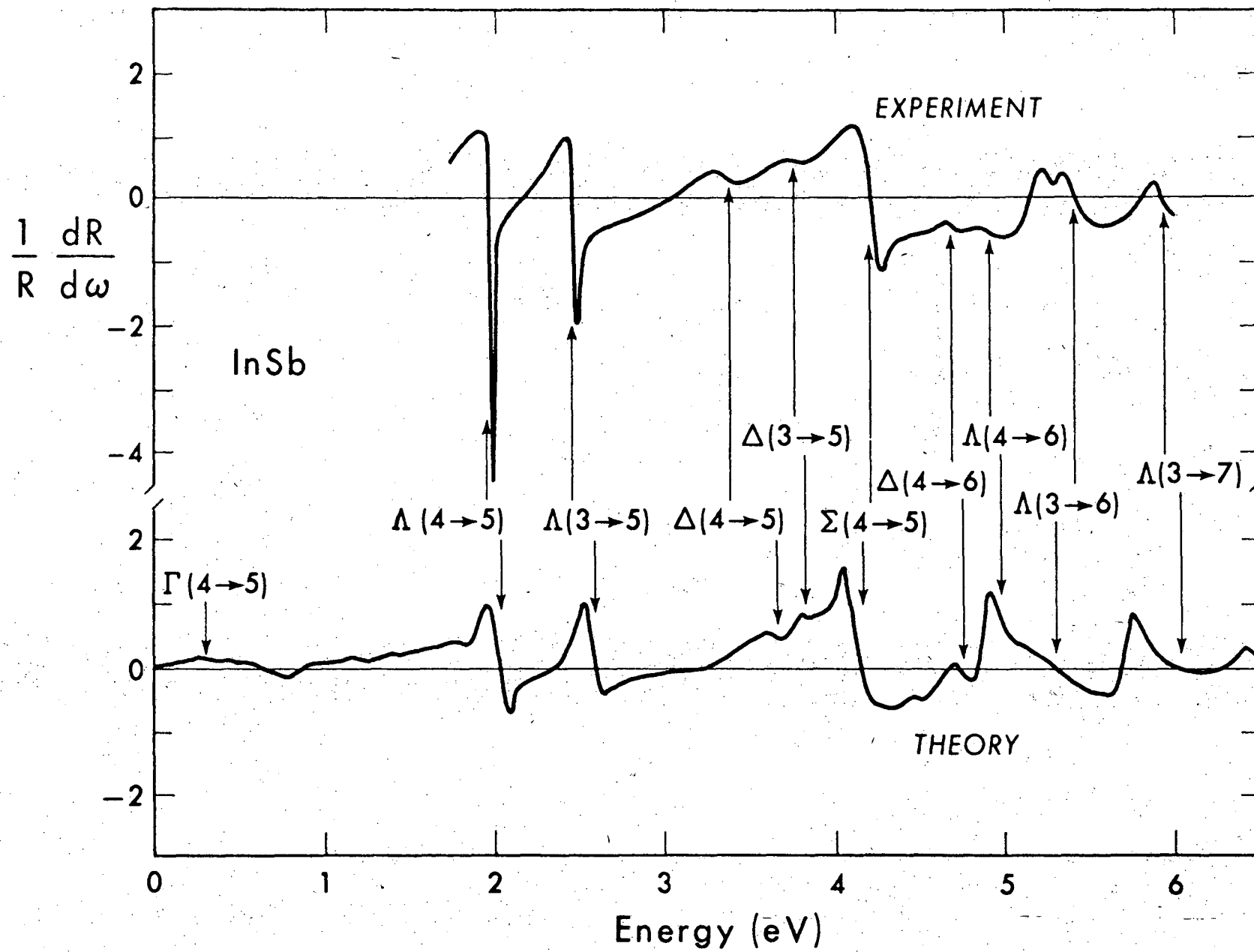


Fig. 8

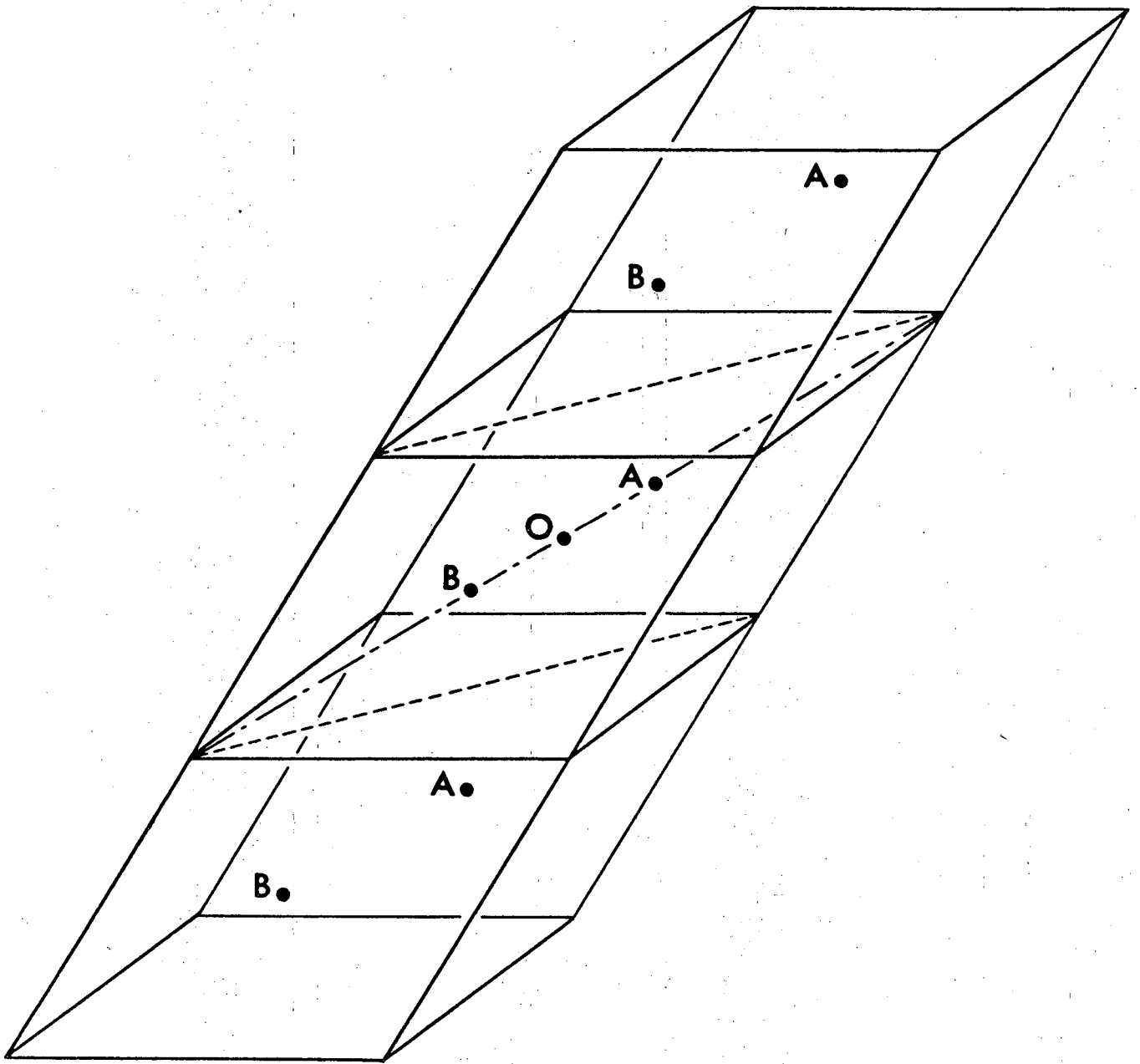


Fig. 9

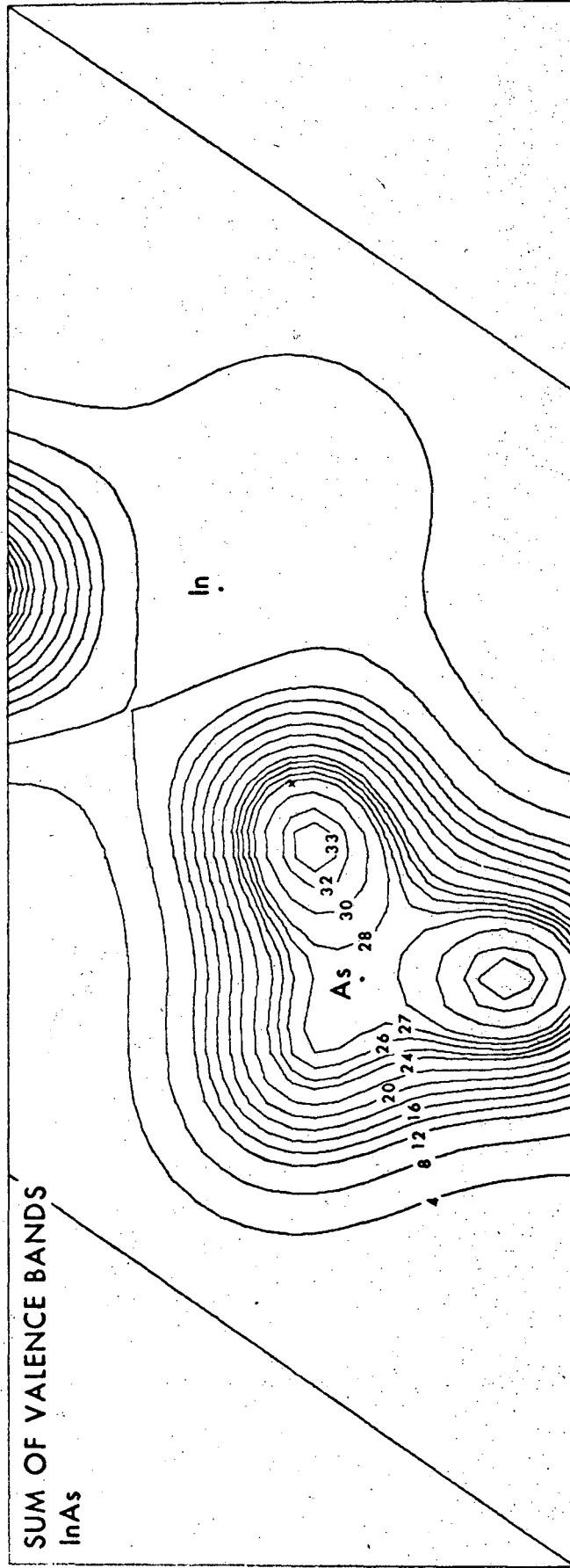


Fig. 10

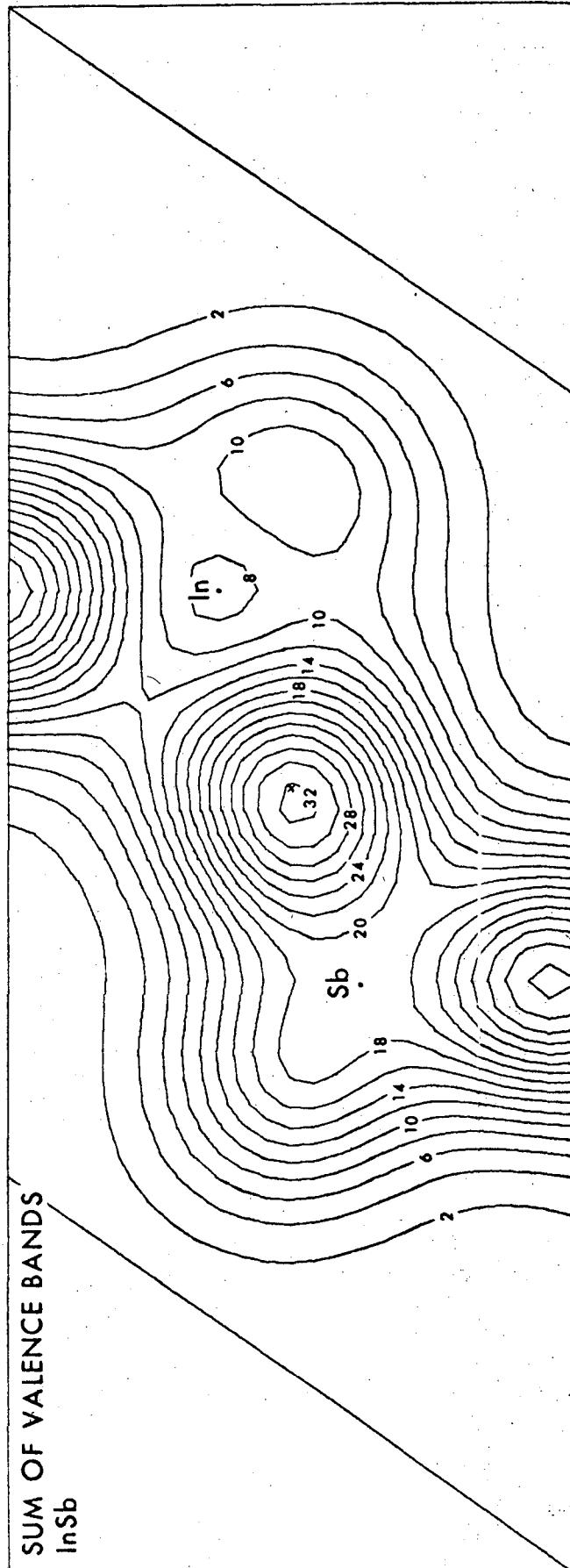


Fig. 11

LEGAL NOTICE

*This report was prepared as an account of work sponsored by the United States Government. Neither the United States nor the United States Atomic Energy Commission, nor any of their employees, nor any of their contractors, subcontractors, or their employees, makes any warranty, express or implied, or assumes any legal liability or responsibility for the accuracy, completeness or usefulness of any information, apparatus, product or process disclosed, or represents that its use would not infringe privately owned rights.*

TECHNICAL INFORMATION DIVISION  
LAWRENCE BERKELEY LABORATORY  
UNIVERSITY OF CALIFORNIA  
BERKELEY, CALIFORNIA 94720